

A biomimetic nanoenzyme for starvation therapy enhanced photothermal and chemodynamic tumor therapy

Keqiang Xu,^{‡a, b} Xiaqing Wu,^{‡a, b} Yan Cheng,^{*a} Jiao Yan,^a Yanlin Feng,^a Rui Chen,^{*c} Runxiao Zheng,^{a, b} Xi Li,^{*d} Panpan Song,^{a, b} Yanjing Wang,^{a, b} and Haiyuan Zhang^{* a, b}

^aLaboratory of Chemical Biology, Changchun Institute of Applied Chemistry, Chinese Academy of Sciences, Changchun, 130022, Jilin, China.

^bUniversity of Science and Technology of China, Hefei, 230026, Anhui, China.

^cCollege of Science, Jilin Provincial Key Laboratory of Human Health Status Identification and Function Enhancement, Changchun University, Changchun, 130022, Jilin, China.

^dSchool of Chemistry and Life Science, Changchun University of Technology, Changchun, 130012, Jilin, China.

[‡]These authors contributed equally to this work.

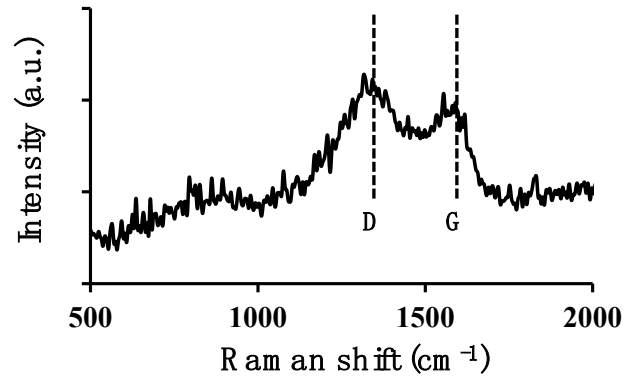


Fig. S1 The typical D and G bands in the Raman spectrum appearing at 1360 and 1580 cm⁻¹ confirmed the existence of carbon in the products.

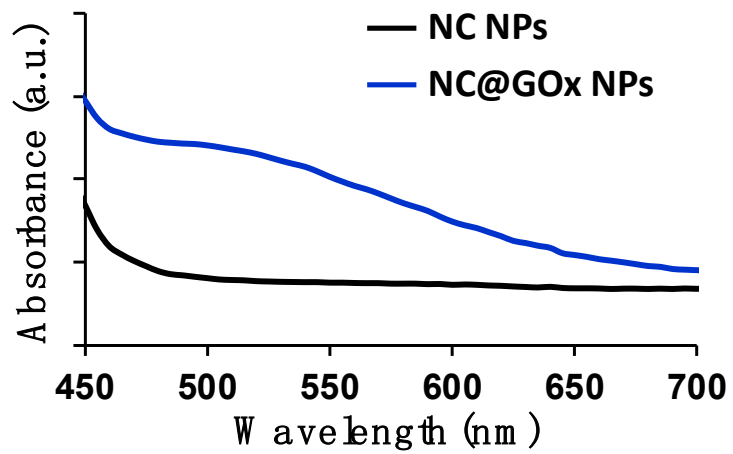


Fig. S2 UV-Vis spectra of hydroxamate-Fe(III) complex which were generated from glucose treated with NC NPs (100 $\mu\text{g}/\text{mL}$) and NC@GOx NPs (100 $\mu\text{g}/\text{mL}$).

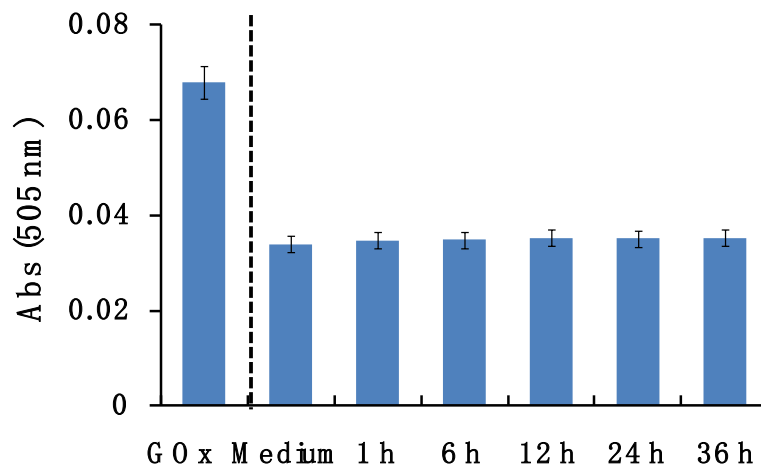


Fig. S3 GOx release detection from NC@GOx NPs. 1 mL of NC@GOx NPs (1 mg mL^{-1}) was suspended in cell culture medium with serum (10 %) for 1, 6, 12, 24 or 36 h. After centrifugation, the amount of GOx in the supernatant was determined by assessment of its generated gluconic acid' amounts, which can react with hydroxylamine and Fe(III) to form a red hydroxamate-Fe(III) complex with a maximum absorbance at 505 nm. Free GOx was used as a positive control and the cell culture medium with serum (10 %) as a negative control. The amount of free GOx was equivalent to that of GOx on NC@GOx NPs.

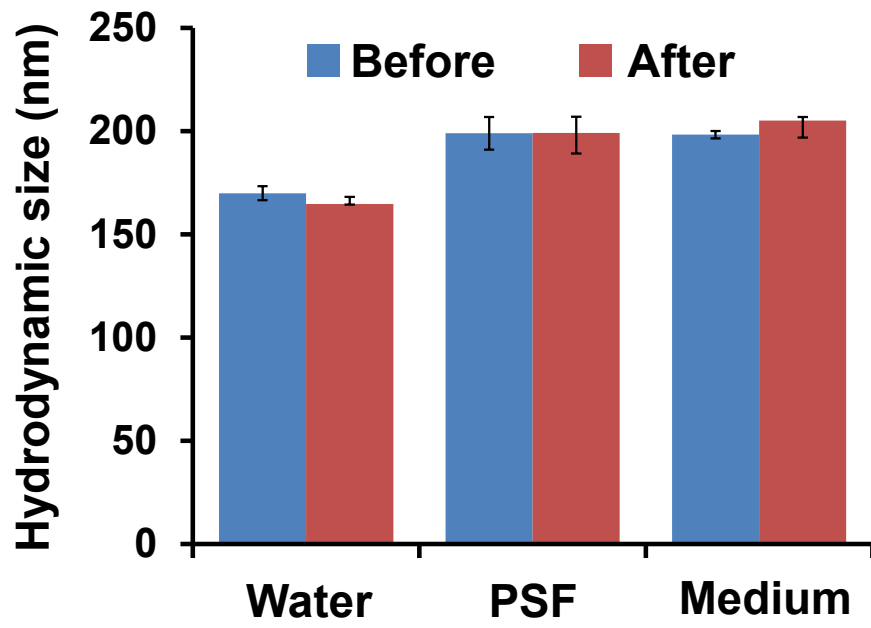


Fig. S4 Hydrodynamic size of NC@GOx dispersed in water, PSF or culture medium before and after 7 days of storage.

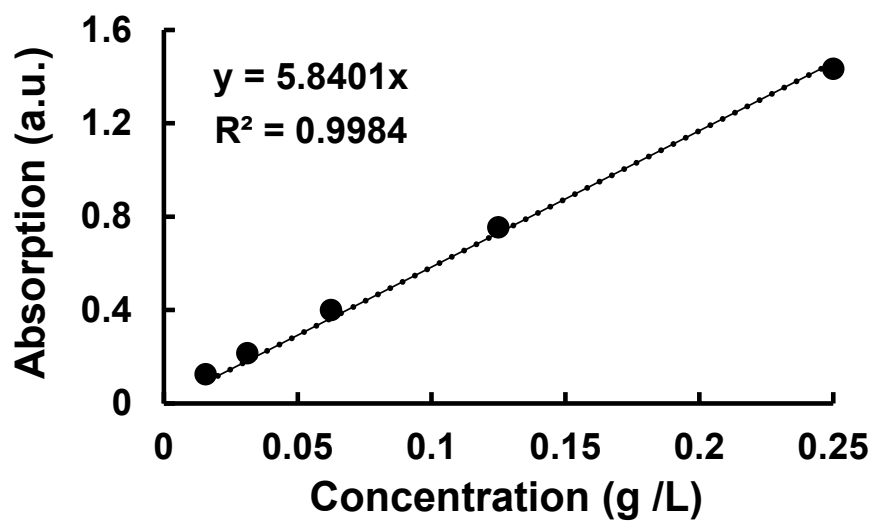


Fig. S5 UV-Vis absorption values and fitting curve of different concentrations of NC@GOx aqueous suspensions at 808 nm.

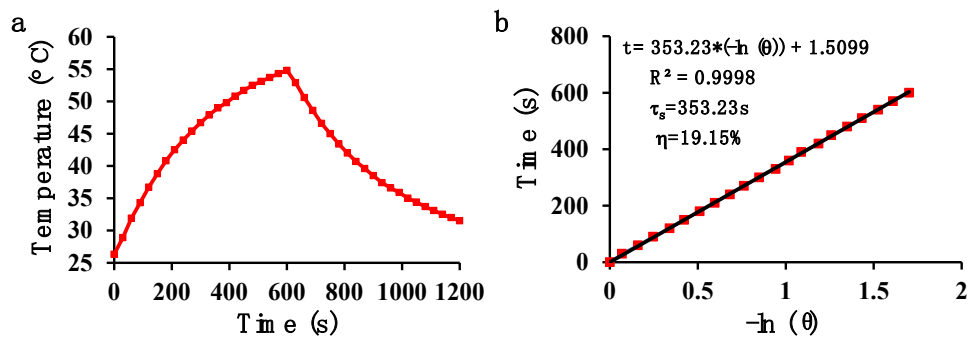


Fig. S6 (a), heating/Cooling curves of NC NPs solution (100 $\mu\text{g}/\text{mL}$) with NIR light irradiation (1 W/cm^2) for 10 min. (b), The plot and linear fit of time versus negative natural logarithm of the temperature increment for the cooling rate.

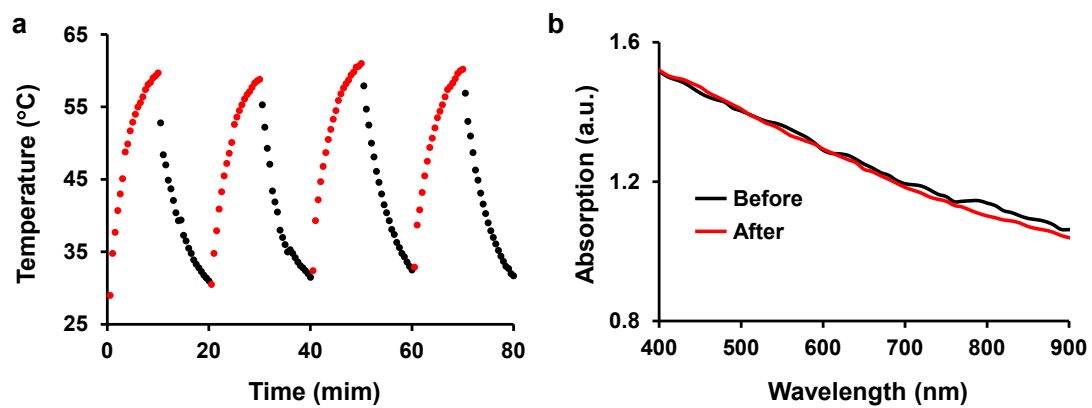


Fig. S7 (a) Photothermal curves of NC@GOx NPs (200 $\mu\text{g}/\text{mL}$) with 808 nm laser irradiation (1.0 W/cm^2 , 10 min for each circle) over five circles; (b) UV-Vis spectra of NC@GOx NPs (200 $\mu\text{g}/\text{mL}$) before and after 808 nm laser irradiation for five circles.

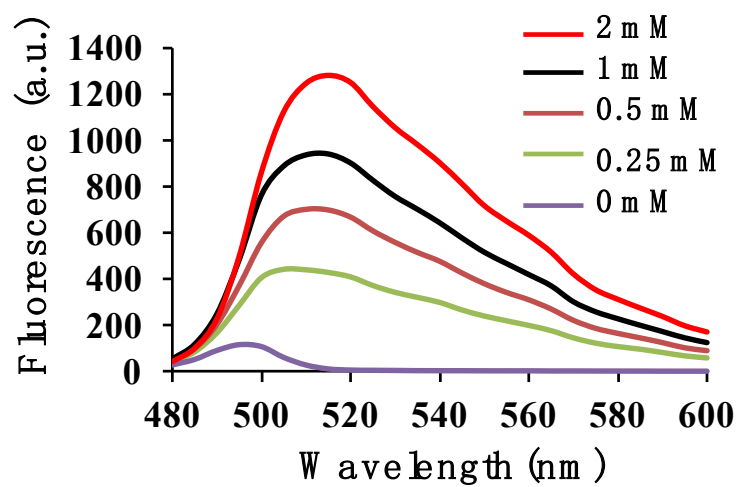


Fig. S8 Hydroxyl radical generation ability on NC@GOx NPs (25 $\mu\text{g}/\text{mL}$) with different concentration of glucose (0-2 mM) by APF assay.

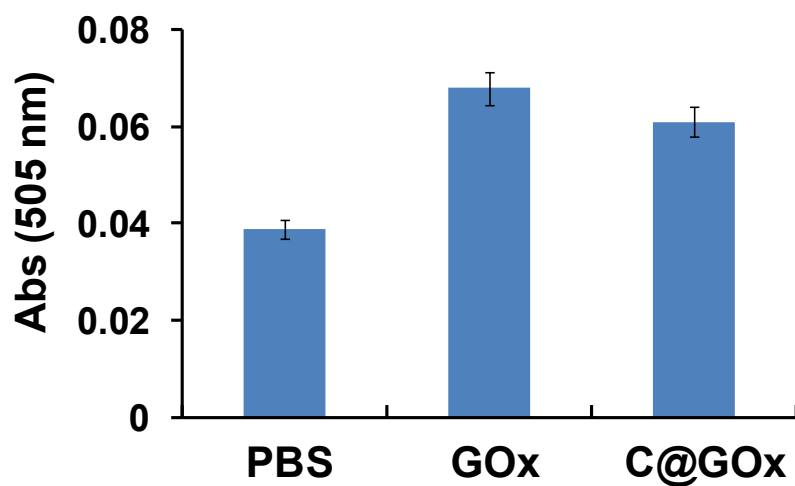


Fig. S9 Comparison of catalytic activities of free GOx and NC@GOx NPs by detecting gluconic acid.

The amount of free GOx was equivalent to that of GOx on NC@GOx NPs. PBS was used as a negative control.

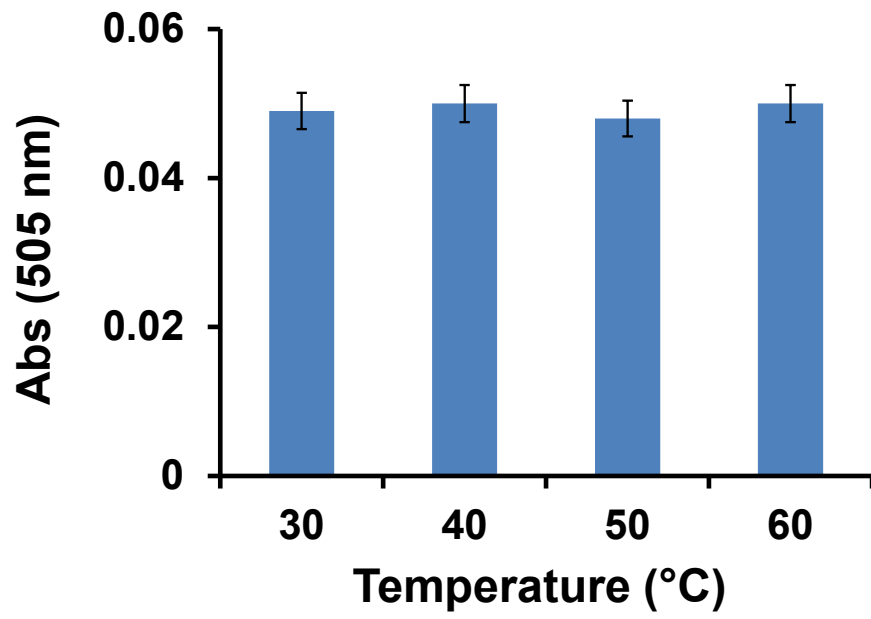


Fig. S10 The catalytic activities of NC@GOx at the temperature range from 30 °C to 60 °C by detecting gluconic acid.

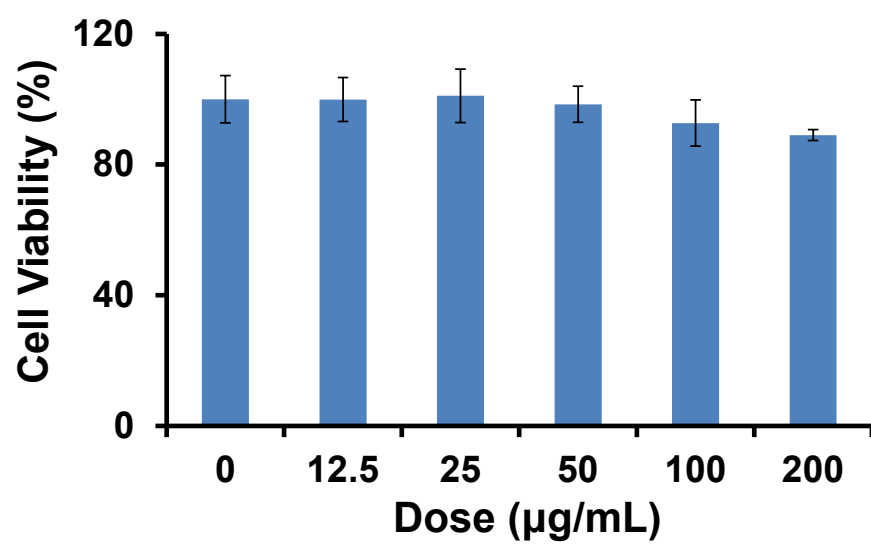


Fig. S11 MTT-based viability assessment of 3T3 cells treated by NC@GOx NPs for 24 h.

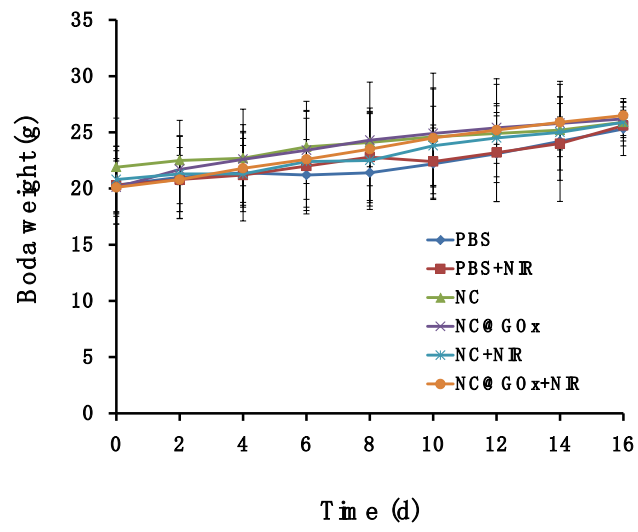


Fig. S12 The weight change curves of mice during the treatment.

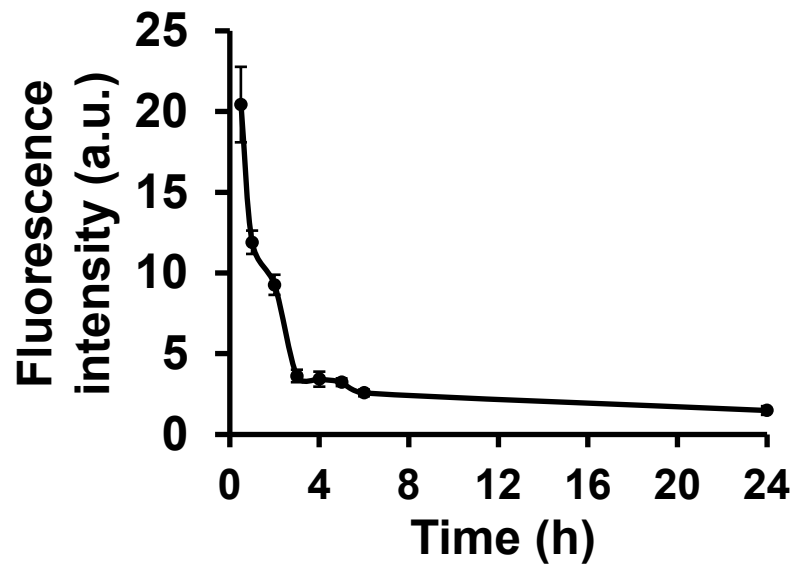


Fig. S13 Blood fluorescence intensity at 0.5, 1, 2, 3, 4, 5, 6 and 24 h post intravenous injection of RhB labeled NC@GOx NPs (20 mg/kg mouse).

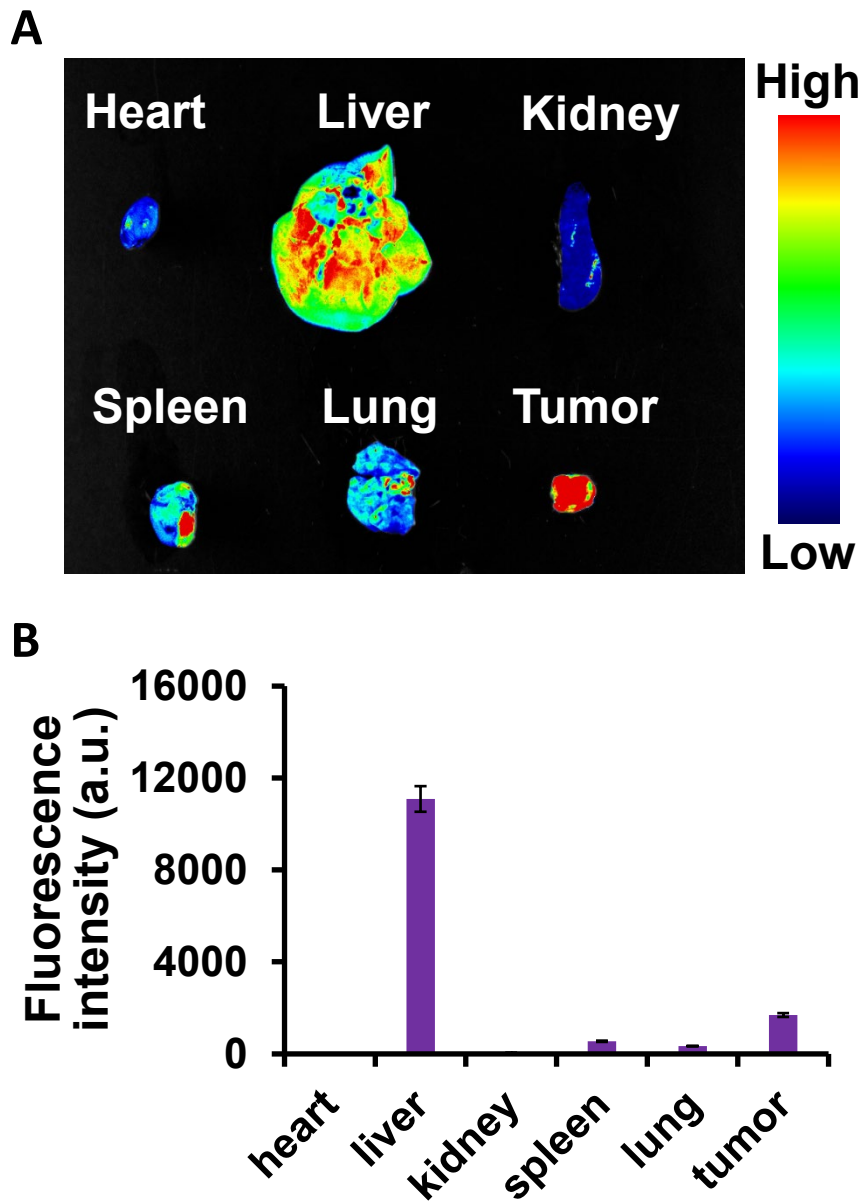


Fig. S14 Ex vivo NC@GOx NPs-biodistribution in isolated tissues from the 4T1 tumor-bearing mice at 24 h post intravenous injection of RhB labeled NC@GOx NPs (20 mg/kg mouse). a. Fluorescence images of heart, liver, spleen, lung, kidney, and tumor. b. Semi-quantitative data of fluorescence intensity from a.